Grey-scale gating for freehand 3D ultrasound

Treece, G.M. Prager, R.W. Gee, A.H. Cash, C.J.C. Berman, L.
Dept. of Eng., Cambridge Univ., UK

This paper appears in: **Biomedical Imaging, 2002. Proceedings. 2002 IEEE International Symposium on**

Publication Date: 7-10 July 2002
On page(s): 993 - 996
ISSN:
Number of Pages: xxxii+1062
Inspec Accession Number: 7522917

Abstract:
Freehand three-dimensional (3D) ultrasound is a flexible imaging technique which allows a 3D data set to be constructed of sequential B-scans from a conventional ultrasound scanner. Since the data is acquired over several seconds, physiological motion generates spatial artifacts in visualisations of the data. Consequently, an electrocardiogram (ECG) signal is often used to gate the acquisition of B-scans to a single point in the cardiac cycle. We present a technique which can remove temporal artifacts by using properties of the grey-scale B-scan data, obviating the need for an external gating signal. B-scans are acquired throughout the cardiac cycle, and any phase can be selected for subsequent visualisation. This enables limited real-time 4D display of the data.

Index Terms:
biomedical ultrasonics blood vessels cardiology data visualisation image sequences medical image processing real-time systems 3D data set B-scan acquisition ECG adult cardiac data arterial data cardiac cycle cardiac cycle single point carotid artery conventional ultrasound scanner data visualisations electrocardiogram signal external gating signal flexible imaging technique freehand 3D ultrasound freehand three-dimensional ultrasound grey-scale B-scan data grey-scale gating limited real-time 4D display physiological motion sequential B-scans spatial artifacts temporal artifacts

Documents that cite this document
There are no citing documents available in IEEE Xplore at this time.

GREY-SCALE GATING FOR FREEHAND 3D ULTRASOUND

G.M. Treece, R.W. Prager, A.H. Gee

Department of Engineering,
University of Cambridge,
Trumpington Street,
Cambridge, UK, CB2 1PZ.

C.J.C. Cash, L. Berman

Department of Radiology,
University of Cambridge,
Addenbrooke's Hospital,
Cambridge, UK, CB2 2QQ.

ABSTRACT

Freehand three-dimensional (3D) ultrasound is a flexible imaging technique which allows a 3D data set to be constructed of sequential B-scans from a conventional ultrasound scanner. Since the data is acquired over several seconds, physiological motion generates spatial artifacts in visualisations of the data. Consequently, an electrocardiogram (ECG) signal is often used to gate the acquisition of B-scans to a single point in the cardiac cycle. We present a technique which can remove temporal artifacts by using properties of the grey-scale B-scan data, obviating the need for an external gating signal. B-scans are acquired throughout the cardiac cycle, and any phase can be selected for subsequent visualisation. This enables limited real-time 4D display of the data.

1. INTRODUCTION

Three-dimensional (3D) ultrasound is a developing imaging modality which enables better visualisation of structure and measurement of volume than conventional 2D ultrasound. There are two differing approaches: a dedicated 3D volume probe can directly record a 3D data set, or multiple images (B-scans) from a conventional 2D probe swept across the volume of interest can be reformatted to generate 3D data.

If the anatomy being scanned is dynamic, e.g. the heart, or pulsating arteries, then the time taken to acquire the data set has a critical bearing on the quality of the data. Dedicated volume probes would seem more appropriate for such applications, since they can acquire many volumes per second [1, 2], fast enough to freeze cardiac (and respiratory) motion during acquisition. However, volume probes are still in their infancy compared to traditional 2D probes, which provide considerably better resolution with an associated improvement in diagnostic potential. 3D probes also restrict the size of the acquired volume.

The alternative, known as *freehand* 3D ultrasound [3], has no such restriction: the probe can be moved in whatever manner is appropriate for the anatomy being scanned. Since the data is acquired from 2D probes, the resolution (at least within the plane of each of the B-scans) is very good. However, motion of the anatomy results in spatial distortion within the 3D data set, since each 'slice' of the volume is acquired at a slightly different time. Such distortion affects the clarity of 3D data sets [4], and also the reliability with which volume measurements can be made from the data [5].

Anatomical motion falls into three broad classes. The effect of *patient movement* can be limited by attaching a coordinate reference to the patient, near to the area under investigation [6]. The location of the 2D probe is then recorded with respect to this, rather than an external, static, reference. *Respiratory motion* can be suppressed by always scanning during a single breath hold, which limits the practical acquisition time to roughly 20 seconds. *Cardiac activity* is the other main source of anatomical motion, and since this is (generally) repetitive, ECG gating can be used to ensure that B-scans used in any single visualisation originate from the same phase of the cardiac cycle [7, 8, 9, 10, 11]. This gating can be applied pre- or post-acquisition; in the latter case, the ECG signal and B-scan data are recorded throughout the cycle, effectively generating an (interleaved) 4D data set.

ECG gating is not without its disadvantages, though. Clearly, it requires additional equipment connected to the patient and an extra data stream input to the computer (in addition to the 2D probe locations and the B-scan images from the ultrasound machine). All three data streams must be temporally calibrated with respect to each other, since the phase of the ECG may not correspond to the pulse in the anatomy being scanned. In some cases, for instance for foetal heart scans, an ECG signal is not available [12]. Hence, alternatives to an ECG have been investigated. For Doppler ultrasound data sets, it is possible to use the Doppler information to gate the data [13]. However, for grey-scale data sets, we would either need to pre-set the cardiac frequency using a Doppler prescan [14], or use a separate source for Doppler gating and for data acquisition [15]. Neither solution is ideal — the first makes an unrealistic assumption of precisely uniform cardiac motion, and the second requires simultaneous use of two ultrasound machines.

We present an algorithm which can gate freehand 3D ultrasound data, post-acquisition, based on information in the data itself. This enables dynamic 4D display of data affected by cardiac motion, with significantly reduced temporal jitter artifacts, and without the need for any additional equipment. A different technique, based on Fourier transforms of sections of the entire image sequence, has been applied to foetal heart scans [12]. In contrast, our technique allows for variations in the cardiac cycle during the scan, and can also be applied to 3D Doppler data sets. We show results here for (adult) cardiac and arterial data.

2. DESCRIPTION

Any cardiac signal derived from grey-scale ultrasound data will inevitably be noisy. Ultrasound data is itself noisy, and only a small part of each B-scan may be pulsing: other parts may even be pulsing with a different phase. In addition, movement of the probe as the volume is scanned will generate changes in the B-scans (since the anatomy is different in each scan) which are more

This work was carried out under EPSRC grant GR/N21062.

0-7803-7584-X/02/$17.00 ©2002 IEEE

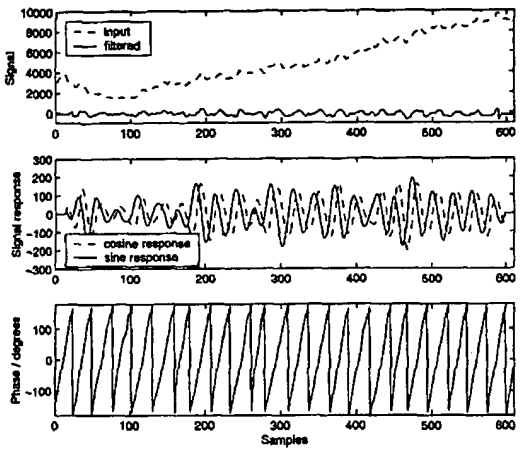

Fig. 1. Estimation of the phase of the input signal. The signal (top, dashed) is first pass-band filtered (top, solid), then the dominant frequency is found. The responses to single period sine and cosine filters at this frequency (middle) are then used to estimate phase at each sample point (bottom).

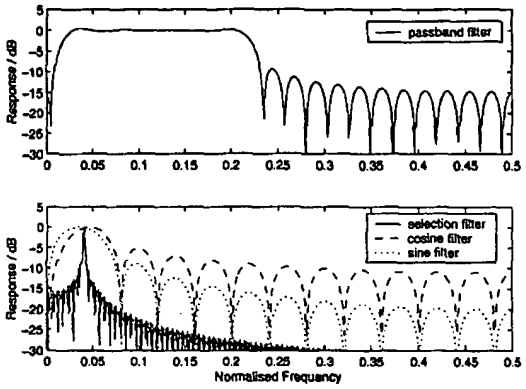

Fig. 2. Filter responses. A linear-phase pass-band filter (top) removes physically implausible cardiac frequencies. Narrow-band filters (bottom, solid) are used to determine the dominant frequency, which defines the broader response sine and cosine filters (bottom, dotted and dashed).

significant than changes caused by cardiac motion. It is therefore vital that we extract as much information as possible out of the grey-scale cardiac signal; we will look at this first, before going on to see how the signal can be derived.

2.1. Extracting cardiac phase from a noisy signal

Figure 1 (top, dashed) shows a typical grey-scale cardiac signal, plotted against the number of the B-scan from which it was derived; a pulse is only barely apparent from this signal. We expect (adult) cardiac signals to vary between 30 and 150 beats per minute, allowing for missed beats and extra systoles. Approximately 25 B-scans are acquired each second, which implies a normalised frequency range (where 1 represents half the sample rate) from 0.04 to 0.2. We can therefore pass-band filter the signal to remove any frequencies clearly outside this range. The filtered signal is shown in Fig. 1 (top, solid), and the filter's frequency response in Fig. 2. Note that this filter has a linear phase response in order not to distort the signal within the pass-band, and a low ripple (0.5dB) to minimise frequency weighting within the pass-band.

The next step is to find the dominant frequency, which we can do simply by using sine transforms of the entire filtered signal. Providing the data set contains multiple cardiac cycles, these have very sharp responses: an example is shown in Fig. 2 (bottom, solid). We cannot simply use this frequency to gate the input data, however, since we expect some variation in cardiac motion throughout the data set. This can be due to slight irregularities in the heart beat, or the result of dropped frames during acquisition[1].

Having found the dominant frequency, we can estimate the phase *at all points in the signal* by filtering it with single period sine and cosine filters at this frequency. The inverse tangent of the output of each of these filters gives an estimate of the phase of the dominant signal. Essentially the same technique can be used for decoding phase modulated signals.

The sine and cosine filters have a broader response than the frequency selection filter, as can be seen in Fig. 2 (bottom, dotted and dashed), and hence can accommodate variation in the frequency of the cardiac waveform. The output of each filter is shown in Fig. 1 (middle), and the resulting phase estimate in Fig. 1 (bottom). In providing the centre frequency for the phase filters, the frequency selection filter can be seen as optimising the amplitude response of the phase filters, and hence the robustness of the phase estimate. In all other respects, the phase estimate is entirely local and independent of the estimate of the dominant frequency.

2.2. Generating a signal containing cardiac information

Using this technique, we can estimate cardiac phase from signals containing limited cardiac information. We could potentially use a deformable mesh [16] or image correlation [17] to track movement in regions of each B-scan. However, these approaches are often expensive in processing time, and are limited by the effect of genuine anatomical changes between B-scans, as mentioned earlier.

In fact, we can adopt a much simpler approach: counting pixels in each B-scan with intensities falling within a user-specified threshold. So long as we constrain the count to within the region of the image affected by cardiac motion (also user-specified), we can generate sufficient information to give a reliable estimate of cardiac phase with which to gate the data.

Figure 3(a) shows one B-scan in a data sequence of the common carotid artery, with the user-specified circular region. The region is generated by simply clicking (to define the centre) then dragging (to change the radius) in the B-scan. Such a region is defined in several B-scans within the sequence, as the location of the carotid artery with respect to the B-scan's origin changes. The region used in any other B-scan is simply the linear interpolation

[1] All algorithms are applied across *acquired frames* rather than *time*. Slight unsteadiness in the acquisition rate therefore results in apparent slight frequency shifts in the signal.

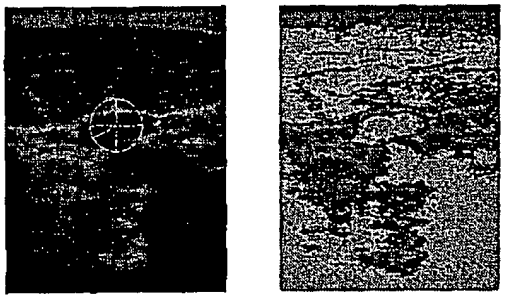

(a) Region of interest (b) Selected threshold

Fig. 3. Signal extraction from grey-scale data: common carotid artery. Image pixels are counted over a user-specified circular region of interest (a) and grey-scale threshold (b).

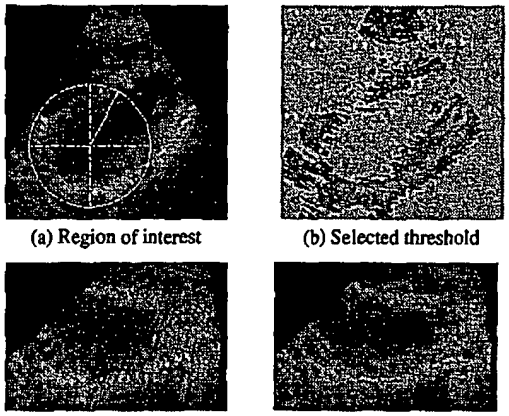

(a) Region of interest (b) Selected threshold

(c) Un-gated reslice (d) Gated reslice

Fig. 5. Grey-scale gating in echocardiographic data. The region of interest in (a) and threshold in (b) have been used to gate a cardiac data set. A reslice through one of the ventricles (c) is dramatically improved by gating (d).

of the centres and radii of the nearest user-defined regions. The user then specifies an intensity range, shown grey in Fig. 3(b). The threshold is chosen to encompass a portion of anatomy whose area changes (at least within the selected region) with cardiac motion.

Having defined the regions and threshold, the number of pixels within the threshold and contained in the region are counted in each B-scan, and this provides the cardiac signal for subsequent phase estimation. Phase can be estimated in just a few seconds, so the user can interactively define the threshold and region to optimise the phase estimate. The signal processing in Sec. 2.1 works equally well for Doppler data, for which the total number of red (moving) pixels can be used to provide the cardiac signal.

Figure 4 (top) shows the display of the cardiac signal: having estimated this, the user determines the centre and range of phases to use in subsequent data visualisation. B-scans within this range are represented by vertical lines drawn on top of the cardiac signal. Visualisation of the data, for instance the reslice in Fig. 4 (bottom), reacts dynamically to the phase sliders, allowing real-time display of the pulsating data.

3. RESULTS

Figure 4 shows a visualisation of a 3D data set of a carotid artery. The threshold, region of interest and resulting signals are as shown in Figs. 3 and 1. The pulsating artifacts in the un-gated data are clearly removed in the gated reslice in Fig. 4(b), where only one B-scan has been used from each cardiac cycle. However, the left hand side of the reslice is now poorly sampled compared to the original data: the probe was being moved too fast at this point.

For reslices gated at maximum contraction or relaxation of the carotid artery, it is possible to use a *group* of B-scans for the visualisation, rather than just one per cycle [18], since here the cross-sectional area is approximately constant for a short period of time. Figure 4(c) shows an example where B-scans with a range of phases have been selected. This clearly improves the resolution of the reslice, while still minimising the motion artifacts.

The technique can also be applied to ultrasound scans of the heart, as demonstrated in Figure 5. Cardiac motion artifacts, clearly evident in the un-gated data in Fig. 5(c), are no longer apparent in the gated data, Fig. 5(d).

Some care is required in the interpretation of the phase estimate in both cases, since it is derived from the varying anatomical data rather than an external ECG at a fixed location. The phase is therefore locked to the deviation of the data across all the recorded B-scans, rather than the actual phase of the cardiac cycle. A phase of zero therefore implies maximal contraction everywhere in the data sequence, rather than, say, the point of systole.

Since our aim is to improve visualisation rather than estimate the cardiac cycle *per se*, this is not a problem. Indeed, it could be argued that for arteries, visualisation at the maximum contraction or relaxation all the way along the artery is ideal. However, the gated visualisation does *not* strictly represent a freeze-frame of the moving anatomy, though in practice it is likely to be very similar, dependent on the setting of the region of interest and threshold.

4. CONCLUSION

We have presented a technique which allows cardiac motion artifacts to be removed from freehand 3D ultrasound images post-acquisition, without any additional equipment. The method requires only a few minutes of user interaction after data acquisition, and can be applied to either grey-scale or Doppler ultrasound data. Initial tests on arterial and cardiac data sets indicate the general applicability of this approach. The phase estimate is also capable of tracking variations in the cardiac cycle. Dynamic (4D) display of the data is possible, but care is required in the interpretation of such displays.

5. REFERENCES

[1] P. Arbeille, V. Eder, D. Casset, L. Quillet, C. Hudelo, and S. Herault, "Real-time 3-D ultrasound acquisition and display for cardiac volume and ejection fraction evaluation," *Ultrasound Med Biol*, vol. 26, no. 2, pp. 201–208, Feb. 2000.

[2] M. S. Sklansky, T. Nelson, M. Strachan, and D. Pretorius, "Real-time three-dimensional fetal echocardiography," *J Ultrasound Med*, vol. 18, pp. 745–752, 1999.

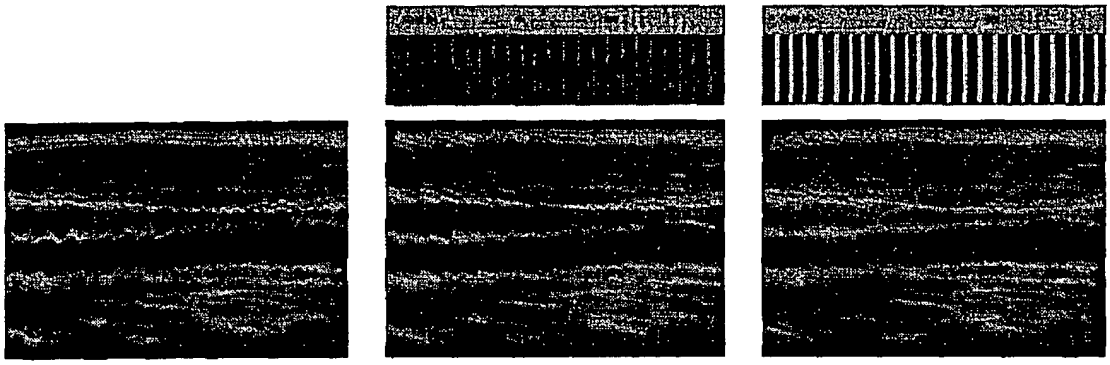

(a) Un-gated reslice (b) Reslice with nearest phase (c) Reslice with phase group

Fig. 4. Effect of grey-scale gating on display: common carotid artery. The bottom row shows reslices orthogonal to the acquired B-scans and the skin surface at the top. The top row shows the user interface for determining the gating phase and range: vertical bars correspond to B-scans included in the reconstruction. (b) A phase range of zero causes the nearest phase B-scan to be selected in each phase group. (c) Wider ranges can be used to involve more B-scans in the reconstruction.

[3] R. W. Prager, A. H. Gee, and L. Berman, "Stradx: real-time acquisition and visualisation of freehand 3D ultrasound," *Med Image Anal*, vol. 3, no. 2, pp. 129–140, 1999.

[4] S. K. Nadkarni, D. R. Boughner, M. Drangova, and A. Fenster, "In vitro simulation and quantification of temporal jitter artifacts in ECG-gated dynamic three-dimensional echocardiography," *Ultrasound Med Biol*, vol. 27, no. 2, pp. 211–222, 2001.

[5] A. Delcker and C. Tegeler, "Influence of ECG-triggered data acquisition on reliability for carotid plaque volume measurements with a magnetic sensor three-dimensional ultrasound system," *Ultrasound Med Biol*, vol. 24, no. 4, pp. 601–605, 1998.

[6] M. L. Chuang, M. G. Hibberd, R. A. Beaudin, M. G. Mooney, M. F. Riley, J. T. Fearnside, and P. S. Douglas, "Patient motion compensation during transthoracic 3-D echocardiography," *Ultrasound Med Biol*, vol. 27, no. 2, pp. 203–209, 2001.

[7] D. C. Barratt, A. H. Davies, A. D. Hughes, S. A. Thom, and K. N. Humphries, "Optimisation and evaluation of an electromagnetic tracking device for high-accuracy three-dimensional ultrasound imaging of the carotid arteries," *Ultrasound Med Biol*, vol. 27, no. 7, pp. 957–968, 2001.

[8] M. Belohlavek, D. A. Foley, J. B. Seward, and J. F. Greenleaf, "3D echocardiography: Reconstruction algorithm and diagnostic performance of resulting images," *Proc SPIE*, vol. 2359, pp. 680–692, 1994.

[9] S. Berg, H. Torp, D. Martens, E. Steen, S. Samstad, I. Høivik, and B. Olstad, "Dynamic three-dimensional freehand echocardiography using raw digital ultrasound data," *Ultrasound Med Biol*, vol. 25, no. 5, pp. 745–753, June 1999.

[10] S. Meairs, J. Beyer, and M. Hennerici, "Reconstruction and visualization of irregularly sampled three- and four-dimensional ultrasound data for cerebrovascular applications," *Ultrasound Med Biol*, vol. 26, no. 2, pp. 263–272, Feb. 2000.

[11] C. Palombo, M. Kozakova, C. Morizzo, F. Andreuccetti, A. Tondini, P. Palchetti, G. Mirra, G. Parenti, and N. G. Pandian, "Ultrafast three-dimensional ultrasound — application to carotid artery imaging," *Stroke*, vol. 29, pp. 1631–1637, Aug. 1998.

[12] M. S. Sklansky, T. R. Nelson, and D. H. Pretorius, "Three-dimensional fetal echocardiography: gated versus nongated techniques," *J Ultrasound Med*, vol. 17, pp. 451–457, 1998.

[13] R. W. Prager, A. H. Gee, M. Pearson, and L. Berman, "Practical segmentation of 3D ultrasound," in *Proc Med Image Understand Anal*, Oxford, UK, 1999, pp. 17–20.

[14] M. Meyer-Wittkopf, N. Rappe, F. Sierra, H. Barth, and S. Schmidt, "Three-dimensional (3-D) ultrasonography for obtaining the four and five-chamber view: comparison with cross-sectional (2-D) fetal sonographic screening," *Ultrasound Obs Gyn*, vol. 15, no. 5, pp. 397–402, 2000.

[15] J. Deng, A. G. Birkett, K. D. Kalache, M. A. Hanson, D. M. Peebles, A. D. Linney, W. R. Lees, and C. H. Rodeck, "Conversion of umbilical arterial doppler waveforms to cardiac cycle triggering signals: a preparatory study for online motion-gated three-dimensional fetal echocardiography," *Ultrasound Med Biol*, vol. 27, no. 1, pp. 51–59, 2001.

[16] F. Yeung, S. F. Levinson, and K. J. Parker, "Multilevel and motion model-based ultrasonic speckle tracking algorithms," *Ultrasound Med Biol*, vol. 24, no. 3, pp. 427–441, 1998.

[17] G. M. Treece, R. W. Prager, A. H. Gee, and L. Berman, "Correction of probe pressure artifacts in freehand 3D ultrasound," in *Med Image Comput Computer-Assist Intervention (MICCAI'01)*, Utrecht, The Netherlands, Oct. 2001, LNCS 2208, pp. 283–290, Springer.

[18] C. P. Allott, C. D. Barry, R. Pickford, and J. C. Waterton, "Volumetric assessment of carotid artery bifurcation using freehand-acquired, compound 3D ultrasound," *Br J Radiol*, vol. 72, pp. 289–292, Mar. 1999.